

# Enhance User Experience of PerfectFit by Resolving Penetrations in the Simulations

Zhengyou Han

zhan26@illinois.edu

## I. INTRODUCTION AND MOTIVATIONS

Clothing is a vital element to our daily life. With the advancements of online shopping and manufacture, the up-rising needs for more accessibility to virtual try-on with customization reveal a great commercial potential. Previous works in this topic usually focus on the customers' experience on fitting themselves in the fixed-shape products, but the new work in the lab, PerfectFit: Custom-Fit Garment Design in Augmented Reality [26], inspires me to explore the interaction method from a different perspective. In PerfectFit, the garments are manipulated and re-designed to fit individuals' physical attributes. Therefore, this new design lowers the barrier of customers' accessibility to stylish products. However, by inspecting the demo frame by frame, I realize there are some improvements can be made to the current phase of PerfectFit.

First, the cloth is not stable. During the demo, we can see the cloth is constantly trembling. Since there lacks the access to the codebase and more related details, I boldly infer the possible reason for this numerical instability might be the inconsistency of motion capture or a non-guaranteed penetration-free algorithm. However, since the cloth remains shaking at the same amplitude when the client role remains still and the incorrect force calculations at 0:44 in the video, I believe the observed instability is more likely to be the typical drawback of position based dynamics. If we can apply an efficient penetration-free simulator in PerfectFit, then it will be closer to an ideal tool in the working scenarios and offers better user experience. Besides, the layers and texture of the garments seems less diverse than expected in real-life situation. Previous works applying learning-based methods have better performance in fast rendering wraps and cloth deformation caused by changing poses. However, the recent methods implemented with real-time simulation are more powerful in handling different materials and objects due to the rigidity to physical laws. Since the combination of cloth is also important in both fashion industry and in our daily life, we can extend PerfectFit to meet broader needs of clothing. In my work, I argue the state-of-art simulator, subspace preconditioned PD-IPC [6], is able to resolve most of the problems in the simulation and implement coupling of other materials and physical effects in the future.



Fig. 1. The unnatural forces and trembling in the demo of PerfectFit

## II. RELATED WORKS

### A. Projective Dynamics

Physical-based cloth simulation has been popular in the realm of graphics community. Modern cloth simulation often endorses implicit time integration scheme pioneered by Baraff and Witkin. [1] Since this scheme will introduce extra damping, strain limiting is also used to counter this problem. Liu et al [2] introduced a new method to simulate the cloth with mass-spring model with implicit Euler and solve it as a energy minimization problem. This idea can be achieved by solving global/local steps alternatively and later is generalized by Bouaziz et al. as Projective Dynamics in their work. [3]

PD is an excellent framework for paralleling due to its design. In each solve, the global steps solve a fixed linear system and remain constant during the solving of local steps. And the local steps are required to solve the constraints inside the system separately in parallel. This alternating procedure continues until the energy converge within an arbitrary tolerance. In previous works, some techniques are applied to enhance the performance of PD such as using Cholesky factorization to precomputed system matrix, applying approximation in global solves by fast Jacobi iterations, and implementing Chebyshev acceleration techniques to accelerate convergence. [4] [5] Unfortunately, it is reported PD still requires a substantial number

of iterations in high-resolution cloth simulation scenarios. [6]

But, PD is still one of the most suitable simulator for parallel and its variants work are proven decent with the contact models will be introduced in the following section. This GPU-friendly feature also unleashes its potential in differentiable simulations for system identification which will be in another topic I am going to discuss later.

### B. Incremental Potential Contact

IPC [?] [31] is a computational approach based on idea of interior-point method. In 1992, Mehrotra incorporated barrier functions to approximate inequality constraints induced by collisions and contact. [29] And Li et al. validated the robustness and feasibility of barrier-based collision models and generalize their idea as Incremental Potential Contact. Traditional contact model in early works tend to formulate collisions as impulses [1] [30] [9]. Doing so will introduce inevitable stiffness to the simulations which requires huge workload on parameter tuning to eliminate undesired artifacts and ensure the convergence. And later, works on complementarity programming also failed in handling collisions in complex scenarios. Since the object is NP-hard, the searching always far more expensive than we can afford. [10] Another popular idea is penalty methods and repulse methods [3] [8] [11] [5] which are inexpensive. But still, they usually fail in larger time steps and intersections among models continuous to exist.

In IPC, the contacts are formulated by barrier function as a form of potential w.r.t. unsigned distance. It brings better robustness and smoothness to the simulation than those rely on signed distance methods and impulses. The barrier penalty function in IPC yields an increasing repulsion when colliding objects move closer and pushes them away before penetration happens. By this mean, interpenetration is avoided in each time step while the algorithm ensures the inequality constraints are constantly satisfied. The Continuous Collision Detection (CCD) is used in line search of IPC. It ensures the displacement update is well confined in domain of the barrier functions. Since CCD-based line search gives the direction for the simulation to continue, CCD is required in every iteration and it is the key element of IPC to keep penetration-free. It converts constrained simulation to unconstrained ones and therefore allows high-resolutions of collisions and contacts. However, since CCD is required in each iteration, it leads to high cost and unfriendliness to parallel. Follow-up works showed possible ways to conquer this challenge. Lan and colleagues [4] alleviated the efficiency issue by applying an inexact approximation to replace the Newton iteration [12] used in original IPC on PD framework and further upgrade it by stencil-wise Newton-CG in their later work. [13] And most recent work by Li et al. formulates a new PD framework focus on subspace simulation and obtained 4x speed up over previous PD-IPC versions as well as a 10x acceleration over original IPC. By Li and colleagues [6], global steps of subspace-PD-IPC will solve for displacement field in subspace to capture low-frequency motion modes with pre-factorized global matrix. And the high frequency details are solved with

Chebyshev-Jacobi relaxation [5] [14] on the full-order system. According to their performance report, this new scheme yields a suitable performance for real-time cloth simulation while maintaining penetration-free. [6] The details of the framework of this work will be discussed in the later section of my proposed method and will be the foundation of it.

Further works on IPC also validates the robustness of IPC in different scenarios such as co-dimensional simulation for thin membranes [21], penetration-free rigid body simulation [17], wrinkle simulation [20] and other materials and effects such as solid-fluid coupling, multi-bodies dynamics and adherent materials simulation. [18] [19] [22]. Now, IPC and its variants are still evolving rapidly with the core idea of keeping penetration-free while aiming for high speed in rich resolution.

### C. Differentiable Cloth Simulation

Differentiable simulation has been an uprising topic in the intersection of computer graphics and machine learning. In differentiable simulation, gradients for initial states, system parameters and design parameters are used to approximate the desired states, usually future states of the system. By this mean, a new type of simulator suitable for real-time simulation and interactive applications seems to have great potential. Recently, there are encouraging breakthroughs in rigid-body dynamics [16] and soft-body dynamics [8] [?]. However, due to the higher requirements in resolution and rich contacts, the attempts for differentiable cloth simulation remain comparably sparse to other topics.

In 2022, Li et al. proposed DiffCloth, a new differentiable cloth simulator, based on dry frictional contact model [7] and embeds it to differentiable PD framework introduced by [15] In model of dry frictional contact, the contacts are assumed only happen to nodes. Therefore, Ly and colleagues [7] formulate the contacts in three situations respectively which are take-off, stick and slip. Li et al. implement this idea in their implicit time integration and further calculate the gradients of velocities. Their gradient-based method and backpropagation are an enhanced version of the work by Du et al. which focus on rigid body with low frequency of contacts and over-simplified frictions. [15] DiffCloth shows strong capability in solving multiple tasks like trajectory prediction and system identification. [24]. DiffCloth is a great success to simulate frictional contact events in cloth, but the work the Yu et al. [17] still shows it fail to strictly avoid undesired artifacts and penetrations. And in their work, Yu et al. claim a decent combination of IPC and DiffCloth and create a new differentiable simulator to solve intersection-free friction contact and two-way coupling with articulated rigid bodies. But, since IPC and its latest variants are still suffering from high computational costs, I think the combination of IPC and differentiable simulation require further research.

In December 2023, Li et al. introduced their new work after DiffCloth, namely DiffAvatar. [27] This work presents a new downstream application of differentiable cloth simulation. DiffAvatar utilizes differentiable simulation to generate physically plausible assets that can be used for simulation applications. In

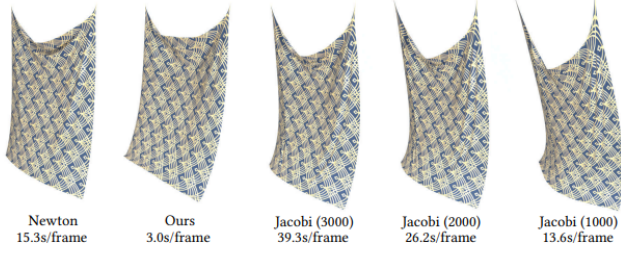


Fig. 2. A comparison between subspace PD-IPC with Chebyshev-Accelerated Jacobi-PD by Wang[2015]. (250K vertices and 500K triangles) [6]

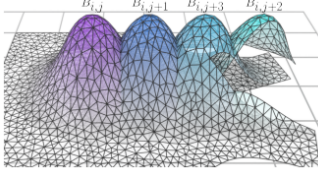


Fig. 3. The illustration of how subspace is built. [6]

their work, DiffAvatar uses scanned body information and 2D garments data successfully build a realistic cloth animation on the avatar with different poses. [27] Different from PerfectFit, DiffAvatar solely focus on the scene recovery from real-time gathered data; while PerfectFit emphasizes the mechanism of interaction between virtual garments and designer. However, I think it is a outstanding example for the implementation of differentiable cloth simulation.

### III. PROPOSED METHOD

My idea is largely constructed upon the subspace-PD-IPC. [6] Therefore, it is helpful to follow framework of this work.

#### A. Construction of Subspace

Subspace simulation is a new idea for IPC and its variant. It is built upon Reduced-Order Modeling and aimed to reduce the critical degrees of freedoms to speedup the simulation. In order to do so, first clothing items are treated as several flat fabric pieces connected with stitches rather than a whole piece of fabric. So, the cloth is defined as  $\Omega = \cup_{i=1}^k \Omega_k$  where  $\Omega$  stands for the domain of patches for 1 to k. Next, Li and colleagues embed the cloth domain onto a 2D Cartesian grid and apply Material Point Method quadratic spline shape functions on the grid points as following. [6]

$$B_{ij}(X) = N(u/\Delta x - i)N(v/\Delta x - j) \quad (1)$$

$$N(x) = \begin{cases} \frac{3}{4} - x^2, & |x| < \frac{1}{2}, \\ \frac{1}{2}(\frac{3}{2} - |x|)^2, & \frac{1}{2} \leq |x| < \frac{3}{2}, \\ 0, & \frac{3}{2} \leq |x|. \end{cases} \quad (2)$$

where (i,j) denotes the grid index, u and v represent the parameterization of X,  $\Delta x$  correspond to spline's kernel size and the spacing of the 2D grid. By this mean, ambient space of  $\Omega$  is decomposed as  $\mathcal{P} = \mathcal{B} \otimes I_3 \in \mathbb{R}^{3M \times 3N}$  which means

space basis matrix  $\mathcal{P}$  is represented by Kronecker product between spline basis  $\mathcal{B}$  and 3D identity matrix where M is the number of bases and N is number of vertices. Now, the states in subspace with given reference position  $x_0$  is expressed as  $\{x : x = x_0 + \mathcal{P}y, y \in \mathbb{R}^{3M}\}$

#### B. Subspace Projective Dynamics

By [6], they sketch the global step upon the optimization time integration outlined by [23] which leads to solving a linear system with fixed system matrix  $\mathbf{H} = \frac{1}{h^2} \mathbf{M} + \mathbf{K}_{\text{mem}} + \mathbf{K}_{\text{bend}}$ , where  $\mathbf{K}_{\text{mem}}$ ,  $\mathbf{K}_{\text{bend}}$  stand for membrane energy Hessian and bending energy Hessian at the rest shape. More specifically, the global solve will focus on solving  $\mathbf{H}u = b$  where  $u$  is the displacement increment respect to previous global step. By restricting the displacement to the form  $u = \mathcal{P}y$ , we can obtain a reduce-order global system as

$$\mathcal{P}^\top \mathbf{H} \mathcal{P} y = \mathcal{P}^\top b. \quad (3)$$

and therefore  $\hat{\mathbf{H}} = \mathcal{P}^\top \mathbf{H} \mathcal{P}$  as reduced global system matrix with a dimension corresponding to the number of bases in  $\mathcal{P}$ .

#### C. Contacts

As mentioned in previous section, the contacts in IPC is handled by barrier-based method. The contact proxy in subspace PD-IPC is defined as

$$\hat{B}(x; x^*) = B(x) + \nabla B(x^*)^\top (x - x^*) + \frac{1}{2} \|x - x^*\|_{\nabla^2 B(x^*)}^2. \quad (4)$$

where  $x^*$  is the initial state and  $B(x)$  is barrier potential function defined as

$$B(x) = \sum_{P,T} b(\text{dist}(P,T)) + \sum_{E_1, E_2} b(\text{dist}(E_1, E_2)) \quad (5)$$

and

$$b(d) = \begin{cases} -(d - \hat{d})^2 \log(d/\hat{d}), & 0 < d < \hat{d}, \\ 0, & d \geq \hat{d}. \end{cases} \quad (6)$$

Here, d and dist are the calculated distance between objects, (P,T) represents an point-triangle part and  $(E_1, E_2)$  represents an edge-edge pair. The computation details can be found in supplementary of IPC by Li et al. [?]

Therefore, the subspace global matrix based on (3) with contacts will be

$$\mathcal{P}^\top (\mathbf{H} + \nabla^2 B(x^*)) \mathcal{P} = \mathcal{P}^\top \mathbf{H} \mathcal{P}^\top + \mathcal{P}^\top \nabla^2 B(x^*) \mathcal{P}^\top \quad (7)$$

Since the global system is subject to constant changes, Li and colleagues endorse BFGS iterations to reuse the global system matrix in non-contact situation. The details of utilization and tuning of BFGS iteration can be find in their work.[Li et al. 2023] Other-than BFGS, the Jacobi iteration is also used in solving global steps on full order.

Since PD solver will provide a trial solution containing penetrations, Li et al. suggest to performe penetration correction by following energy minimization. This step can be helped with Newton-PCG.

$$\frac{1}{2h^2} \|x - x^{\text{tr}}\|_M^2 + B(x). \quad (8)$$



Fig. 4. A high-resolution (more than 120k) simulation carried out by subspace IPC which is strictly non-penetration. The average cost is 23s per frame. [6]

where  $x^{\text{tr}}$  denotes the trail solution.

In conclusion, subspace-PD-IPC has an algorithm as following: And in order to fuse it into PerfectFit, we can sketch

---

**Algorithm 1** Subspace PD-IPC

---

```

if it is the first time step then
    Construct subspace basis sparse matrix.  $\mathcal{P}$ .  $\triangleright$  Section III.A
    Factorize the global matrix  $\mathcal{P}^\top \mathbf{H} \mathcal{P}$ .  $\triangleright$  (3)
end if
Update prediction position.  $\hat{x}$ 
Run global step w.o. contact at  $\hat{x}$ 
Construct contact proxy.  $\triangleright$  Section III.C
Initialize BFGS history.
while not converged do
    Run 2 iterations of subspace BFGS.
    Run 5 iterations of Jacobi on full order.
    Local steps solved in parallel.
end while
Run penetration correction step.  $\triangleright$  Section III.C

```

---

an algorithm based on Algorithm 1.

---

**Algorithm 2** Proposed Algorithm

---

```

if Garment is modified then
    Read and build meshes
    Construct new subspace and update basis sparse matrix  $\mathcal{P}$  based on current states
    Run Algorithm 1
end if
Update meshes w.r.t. motions of clients
Run Algorithm 1

```

---

#### D. A brief of DiffAvatar

The pipeline of DiffAvatar consists of three major parts which are preprocessing, forward computation and backward propagation.

1) *Preprocessing*: Like in PerfectFit, DiffAvatar also uses visual data as input. The visual data is generated by a multi-view capture and used to establish the initial pose and shape of parametric body model.

*Garments and body models*. Garments in DiffAvatar are stored in 2D pattern space at their rest states and modeled as sewn-up triangle meshes in 3D. The body model is combined with the skeleton and the shape information. The skeleton is

described with parameter  $P$  generated by joint angles  $\psi$  and bone lengths with local transformation; the shape is encoded by the statistical shape coefficient  $\nu$  as  $V_0 + \nu V$ , where  $V_0$  and  $V$  encode average body shape and shape basis function respectively. The overall representation of body shape  $S$  can be abstracted as following. [27]

$$S = \mathbb{R}^{3 \times V_b} \times \mathbb{R}^P \rightarrow \mathbb{R}^{3 \times V_b} \quad (9)$$

*Initialization*. In initialization part, Li and her colleagues process multi-view images to reconstruct and segment a 3D scan to initialize the shape and pose of body model. The garment of interest is chosen within the garment class produced by cloth segmentation algorithm ran on each of the cameras. The consistency of the garment class is enforced by selecting the garment classes appear in majority of the cameras. [27]

2) *Forward computation*: In differentiable simulation, the forward computation usually is the simulation from time step  $n$  to  $n + 1$ . So is in DiffAvatar.

*Cloth simulation*. Due to the consideration of efficiency, Li et al. choose XPBD as their simulation model. The update steps is sketched as following. [26]

$$\mathbf{x}_{n+1} = \mathbf{x}_n + \Delta \mathbf{x}_C + \Delta t (\mathbf{v}_n + \Delta t \mathbf{M}^{-1} \mathbf{f}_{ext}) \quad (10)$$

in which  $\mathbf{x}_n$  stands for vertices coordinate at time step  $n$ ;  $\Delta \mathbf{x}_C$  is the sum up displacement after solve constraints in triangle, dihedral, cloth-body collision, cloth-cloth collision.;  $\mathbf{v}_n$  is the velocity at time step  $n$ ;  $\mathbf{M}$  is the mass matrix and  $\mathbf{f}_{ext}$  is external forces. Furthermore, the velocity at time step  $n + 1$  in DiffAvatar is updated as

$$\mathbf{v}_{n+1} = \frac{1}{\Delta t} (\mathbf{x}_{n+1} - \mathbf{x}_n) \quad (11)$$

3) *Backward propagation and optimizations*: The efficient computation of gradient information of  $\theta$  is the key part of differentiable simulation. In DiffAvatar, the backpropagation is described as the minimization of the gradient of goal function  $\phi$  to  $\theta$ , where  $\theta$  is the control parameter vector. The computation of gradient is sketched as following, the details of it is presented in the previous work DiffXPBD. [27] [28]

$$\frac{d\phi}{d\theta} = \frac{\partial \phi}{\partial Q} \frac{dQ}{d\theta} + \frac{\partial \phi}{\partial \theta} \quad (12)$$

where  $Q$  is a sequence containing arbitrary number of previous states and current state. In DiffXPBD and DiffAvatar, (12) is optimized by a replacement of  $Q$  with a adjoint state set  $Q'$ . However, the underlying logic are the same. This optimization only influences the efficiency of the computation. [28]

Now, how to form the parameters  $\theta$  and  $\psi$  is the main issue in this part. DiffAvatar divides the optimization into three categories: body shape and pose optimization, garment pattern optimization and material property estimation. Therefore, the parameters should include the body shape coefficient  $\nu$  and pose (joint angle parameter mentioned above) coefficient  $\psi$ , the control cage coefficient  $\zeta$  and the material parameter  $\lambda$ .  $\zeta$  is very important.  $\zeta$  is a set of vertices on the boundary of 2D garment, and they are chosen to control the deformation and



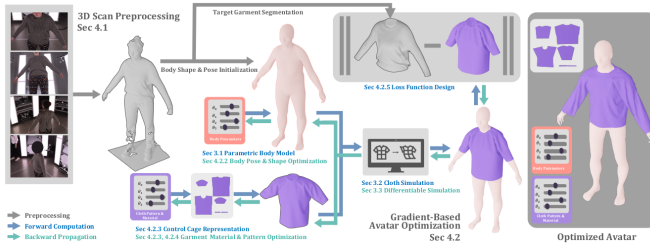


Fig. 5. Pipeline of DiffAvatar. I believe it will help the understanding. [26]

manipulation of 2D patterns. Li et al. emphasize  $\zeta$  prevents ill-shaped or non-physical inverted rest shape geometries from failing the simulation and also avoid the optimization stuck in local minimum. [26] The other two parameters can be explained by their names. Therefore,  $\frac{dQ}{d\theta}$  in (12) can be solved as the sum of the respective derivatives of the displacements of resolving cloth-body collision, triangle constraints, dihedral constraints to parameters in  $\theta$ . [26]

The goal function  $\psi$  is also called loss function. In DiffAvatar, the loss function is formed by feature matching and regularization. Feature matching is aimed to show how well garment matches the scanned data. It is unified by two loss, namely the boundary loss and the interior loss. Boundary loss is to measure if garment is overlapping well enough and interior loss matches the looseness of the fit; as for regularization loss, it is a measure of how well the patterns are maintained during the fitting. [26]

4) *Summary for DiffAvatar*: Li et al. claim DiffAvatar is so far the SOTA algorithm in scene recovery for cloth simulation. [26] The reason I mention this work in my proposal is not for direct implementation of DiffAvatar in PerfectFit. I think it offers a totally different perspective to cope with the issue in PerfectFit. In the first part of my proposal, I attempt to solve the problem by replacing the simulation model while DiffAvatar inspires me to focus more on generating a better assets before utilization of them in the further applications.

#### IV. SUMMARY

In this proposal, I manage to propose a method to optimize the PerfectFit from simulation perspective. I believe IPC and its variants are suitable for the time-sensitive and interactive cloth simulations since the realistic visual effects and diverse materials choices will surely improve the experience for both designers and customers. And I will continue to focus on the advancements in real-time simulation and apply it to more interactive scenarios.

#### REFERENCES

- [1] David Baraff and Andrew Witkin. 1998. Large steps in cloth simulation. In Proceedings of the 25th annual conference on Computer graphics and interactive techniques. 43–54.
- [2] Tiantian Liu, Adam W. Bargteil, James F. O’Brien, and Ladislav Kavan. 2013. Fast Simulation of Mass-Spring Systems. ACM Trans. Graph. 32, 6, Article 214 (Nov.2013), 7 pages.

- [3] Sofien Bouaziz, Sebastian Martin, Tiantian Liu, Ladislav Kavan, and Mark Pauly. 2014. Projective Dynamics: Fusing Constraint Projections for Fast Simulation. ACM Trans. Graph. 33, 4, Article 154 (July 2014), 11 pages. <https://doi.org/10.1145/2601097.2601116>
- [4] Lei Lan, Guanqun Ma, Yin Yang, Changxi Zheng, Minchen Li, and Chenfanfu Jiang. 2022b. Penetration-free projective dynamics on the GPU. ACM Transactions on Graphics (TOG) 41, 4 (2022), 1–16
- [5] Huamin Wang. 2015. A chebyshev semi-iterative approach for accelerating projective and position-based dynamics. ACM Transactions on Graphics (TOG) 34, 6 (2015), 1–9.
- [6] Xuan Li, Yu Fang, Lei Lan, Huamin Wang, Yin Yang, Minchen Li, Chenfanfu Jiang. 2023. Subspace-Preconditioned GPU Projective Dynamics with Contact for Cloth Simulation. ACM Transactions on Graphics (SIGGRAPH Asia)
- [7] Mickaël Ly, Jean Jouve, Laurence Boissieux, and Florence Bertails-Descoubes. 2020. Projective Dynamics with Dry Frictional Contact. ACM Trans. Graph. 39, 4, Article 57 (July 2020), 8 pages. M. Macklin, K. Erleben, M
- [8] Moritz Geilinger, David Hahn, Jonas Zehnder, Moritz Bäcker, Bernhard Thomaszewski, and Stelian Coros. 2020. ADD: analytically differentiable dynamics for multi-body systems with frictional contact. ACM Transactions on Graphics (TOG) 39, 6 (2020), 1–15
- [9] Rachel Weinstein, Joseph Teran, and Ronald Fedkiw. 2006. Dynamic simulation of articulated rigid bodies with contact and collision. IEEE Transactions on Visualization and Computer Graphics 12, 3 (2006), 365–374.
- [10] Mihai Anitescu and Florian A Potra. 1997. Formulating dynamic multi-rigid-body contact problems with friction as solvable linear complementarity problems. Nonlinear Dynamics 14, 3 (1997), 231–247.
- [11] Miles Macklin, Kenny Erleben, Matthias Müller, Nuttapong Chentanez, Stefan Jeschke, and Tae-Yong Kim. 2020. Primal/dual descent methods for dynamics. In Computer Graphics Forum, Vol. 39. Wiley Online Library, 89–100.
- [12] Rahul Narain, Matthew Overby, and George E Brown. 2016. ADMM projective dynamics: fast simulation of general constitutive models.. In Symposium on Computer Animation, Vol. 1. 2016.
- [13] Lei Lan, Minchen Li, Chenfanfu Jiang, Huamin Wang, and Yin Yang. 2023. Second-order Stencil Descent for Interior-point Hyperelasticity. ACM Transactions on Graphics (TOG) (2023)
- [14] Andy Wathen. 2008. Chebyshev Semi- iteration in Preconditioning. Technical Report. Steffen Wiewel, Moritz Becher, and Nils Thuerey. 2019. Latent space physics: Towards learning the temporal evolution of fluid flow. In Computer graphics forum, Vol. 38. Wiley Online Library, 71–82
- [15] Tao Du, Kui Wu, Pingchuan Ma, Sebastien Wah, Andrew Spielberg, Daniela Rus, and Wojciech Matusik. 2021. DiffPD: Differentiable Projective Dynamics. ACM Trans. Graph. 41, 2, Article 13 (Oct. 2021), 21 pages. <https://doi.org/10.1145/3490168>
- [16] Jie Xu, Tao Chen, Lara Zlokapa, Michael Foshey, Wojciech Matusik, Shinjiro Sueda, and Pulkit Agrawal. 2021. An End-to-End Differentiable Framework for ContactAware Robot Design. In Proceedings of Robotics: Science and Systems. Virtual. <https://doi.org/10.15607/RSS.2021.XVII.008>
- [17] Yu, Xinyuan and Zhao, Siheng and Luo, Siyuan and Yang, Gang and Shao, Lin. 2023. DiffClothAI: Differentiable Cloth Simulation with Intersection-free Frictional Contact and Differentiable Two-way Coupling with Articulated Rigid Bodies. IEEE/RSJ International Conference on Intelligent Robots and Systems (IROS). Unpublished.
- [18] Tianyi Xie, Minchen Li, Yin Yang, Chenfanfu Jiang. 2023. A Contact Proxy Splitting Method for Lagrangian Solid-Fluid Coupling. ACM Transactions on Graphics (SIGGRAPH)
- [19] Yunuo Chen\*, Minchen Li\* (equal contributions), Lei Lan, Hao Su, Yin Yang, Chenfanfu Jiang. A Unified Newton Barrier Method for Multi-body Dynamics. 2022. ACM Transactions on Graphics Volume 41 Issue 4 Article No.: 66pp 1–14. <https://doi.org/10.1145/3528223.3530076>
- [20] Yunuo Chen, Tianyi Xie, Cem Yuksel, Danny Kaufman, Yin Yangm Chenfanfu Jiang, Minchen Li. 2023. Multi-Layer Thick Shells. ACM SIGGRAPH 2023 Conference Proceedings (July) 2023 Article No.: 25Pages 1–9 <https://doi.org/10.1145/3588432.3591489>
- [21] Minchen Li, Danny M. Kaufman, Chenfanfu Jiang. 2021 Codimensional incremental potential contact. ACM Transactions on Graphics Volume 40 Issue 4 Article No.: 170pp 1–24, <https://doi.org/10.1145/3450626.3459767>

- [22] Yu Fang\*, Minchen Li\* (equal contributions), Yadi Cao, Xuan Li, Joshua Wolper, Yin Yang, Chenfanfu Jiang. 2023. Augmented Incremental Potential Contact for Sticky Interactions. *IEEE Transactions on Visualization and Computer Graphics (TVCG)*.
- [23] Miklos Bergou, Max Wardetzky, David Harmon, Denis Zorin, and Eitan Grinspun. 2006. A quadratic bending model for inextensible surfaces. In *Symposium on Geometry Processing*. 227–230.
- [24] Yifei Li, Tao Du, Kui Wu, Jie Xu, Wojciech Matusik. 2022. DiffCloth: Differentiable Cloth Simulation with Dry Frictional Contact. *ACM Transactions on Graphics*. Volume 42. Issue 1. Article No.: 2pp 1–20. <https://doi.org/10.1145/3527660>
- [25] Junbang Liang, Ming Lin, and Vladlen Koltun. 2019. Differentiable Cloth Simulation for Inverse Problems. In *Advances in Neural Information Processing Systems*, H. Wallach, H. Larochelle, A. Beygelzimer, F. d’Alché-Buc, E. Fox, and R. Garnett (Eds.), Vol. 32. Curran Associates, Inc. <https://proceedings.neurips.cc/paper/2019/file/28f0b864598a1291557bed248a998d4e-Paper.pdf>
- [26] Akihiro Kiuchi, Anran Qi, Eve Mingxiao Li, Dávid Maruscák, Christian Sandor, and Takeo Igarashi. 2023. PerfectFit: Custom-Fit Garment Design in Augmented Reality. In *SIGGRAPH Asia 2023 XR (SA XR ’23)*, December 12–15, 2023, Sydney, NSW, Australia. ACM, New York, NY, USA, 2 pages. <https://doi.org/10.1145/3610549.3614592>
- [27] Yifei Li, Hsiao-yu Chen, Egor Larionov, Nikolaos Sarafianos, Wojciech Matusik and Tuur Stuyck. 2023. DiffAvatar: Simulation-Ready Garment Optimization with Differentiable Simulation. preprint, arXiv:2311.12194 [cs.CV], <https://doi.org/10.48550/arXiv.2311.12194>
- [28] Tuur Stuyck and Hsiao-yu Chen, 2023. DiffXPBD : Differentiable Position-Based Simulation of Compliant Constraint Dynamics *Proceedings of the ACM on Computer Graphics and Interactive Techniques* Volume 6 Issue 3 Article No.: 51pp 1–14
- [29] Sanjay Mehrotra, 1992. On the Implementation of a Primal-Dual Interior Point Method, *SIAM Journal on Optimization*, Volume 2, No.:4. Pages 575–601.
- [30] Matthew Moore, Jane Wilhelms, 1988, Collision Detection and Response for Computer Animation, *ACM SIGGRAPH Computer Graphics* Volume 22 Issue 4pp 289–298 <https://doi.org/10.1145/378456.378528>
- [31] Minchen Li and Zachary Ferguson and Teseo Schneider and Timothy Langlois and Denis Zorin and Daniele Panozzo and Chenfanfu Jiang and Danny M. Kaufman, 2020. Incremental Potential Contact: Intersection- and Inversion-free Large Deformation Dynamics. *ACM Trans. Graph. (SIGGRAPH)* Volume 39 No.:4
- [32] M. Li, Z. Ferguson, T. Schneider, T. Langlois, D. Zorin, D. Panozzo, C. Jiang, D. M. Kaufman, Incremental 34 potential contact: Intersection- and inversion-free, large-deformation dynamics, *ACM Transactions on Graphics* 39 (4) (2020)